CHEMISTRY
A EUROPEAN JOURNAL

DOI: 10.1002/chem.200601369

Structure, Formation, and Dynamics of Mo_{12} and Mo_{16} Oxothiomolybdenum Rings Containing Terephtalate Derivatives

Jean-François Lemonnier,[a] Sébastien Floquet,*[a] Jérôme Marrot,[a] Emmanuel Terazzi,[b] Claude Piguet,[b] Philippe Lesot,[c] André Pinto,[d] and Emmanuel Cadot*[a]

Abstract: The influence of rigid or semirigid dicarboxylate anions, terephtalate ($TerP^{2-}$), isophtalate ($IsoP^{2-}$), and phenylenediacetate (PDA^{2-}) on the self-condensation process of the $[Mo_2O_2S_2]^{2+}$ dioxothio cation has been investigated. Three new molybdenum rings, $[Mo_{12}O_{12}S_{12}(OH)_{12}(TerP)]^{2-}$ ($[Mo_{12}TerP]^{2-}$), $[Mo_{16}O_{16}S_{16}(OH)_{16}(H_2O)_4(PDA)_2]^{4-}$ ($[Mo_{16}(PDA)_2]^{4-}$), and $[Mo_{16}O_{16}S_{16}(OH)_{16}(H_2O)_2(IsoP)_2]^{4-}$ ($[Mo_{16}(IsoP)_2]^{4-}$) have been isolated and unambiguously characterized in the solid state by single-crystal X-ray studies and in solution by various NMR methods and especially by diffusion-correlated NMR (^1H DOSY) spectroscopy, which was shown to be a powerful tool for the characterization and speciation of templated molybdenum ring systems in solution. Characterization by FT-IR and elemental analysis are also reported. The dynamic and thermodynamic properties of both the sixteen-membered rings were studied in aqueous medium. Specific and distinct behaviors were revealed for each system. The $IsoP^{2-}/[Mo_2O_2S_2]^{2+}$ system gave rise to equilibrium, involving mono-templated $[Mo_{12}IsoP]^{2-}$ and bis-templated $[Mo_{16}(IsoP)_2]^{4-}$ ions. Thermodynamic parameters have been determined and showed that the driving-force for the formation of the $[Mo_{16}(IsoP)_2]^{4-}$ is entropically governed. However, whatever the conditions (temperature, proportion of reactants), the $PDA^{2-}/[Mo_2O_2S_2]^{2+}$ system led only to a single compound, the $[Mo_{16}(PDA)_2]^{4-}$ ion. The latter exhibits dynamic behavior, consistent with the gliding of both the stacked aromatic groups. Stability and dynamics of both Mo_{16} rings was related to weak hydrophobic or π–π stacking inter-template interactions and inner hydrogen-bond network occurring within the $[Mo_{16}(IsoP)_2]^{4-}$ and $[Mo_{16}(PDA)_2]^{4-}$ ions.

Keywords: carboxylate ligands · molybdenum · NMR spectroscopy · polyoxometalates · sulfur

Introduction

The design and the synthesis of nanoscopic inorganic clusters containing a large number of metal centers represent a fantastic challenge. This is because polyoxometalates (POMs) constitute a rich family of numerous and diverse examples of nanoscale objects with spherical, ring, or modular components that are potentially attractive for catalysis,[1–5] medicine,[6–8] magnetism,[9–11] analytical,[12] or supramolecular chemistry.[13–18] In this context, transition-metal ring-like clusters based on the self-condensation of $[Mo_2O_2S_2]^{2+}$ oxothio cation have been investigated for many years.[19,20] This system was shown to be fruitful for developing extended cyclic inorganic clusters, differing in their nuclearity and shape by the nature of the encapsulated substrate, being either mono- or polyphosphates,[21–23] metalates,[24–26] or polycarboxylates.[27–29] The flexible and adaptable cyclic oxothiomolybdenum rings exhibiting an open inner available cavity, display attractive properties for bioin-

[a] J.-F. Lemonnier, Dr. S. Floquet, Dr. J. Marrot, Prof. Dr. E. Cadot
Institut Lavoisier de Versailles, UMR 8180
University of Versailles
45 avenue des Etats-Unis, 78035 Versailles (France)
Fax: (+33) 139-254-381
E-mail: sebastien.floquet@chimie.uvsq.fr
emmanuel.cadot@chimie.uvsq.fr

[b] Dr. E. Terazzi, Prof. Dr. C. Piguet
Department of Inorganic, Analytical and Applied Chemistry
University of Geneva
30 quai E. Ansermet, 1211 Geneva 4 (Switzerland)

[c] Dr. P. Lesot
ICMMO, UMR 8182, Laboratoire de Chimie Structurale Organique
University of Paris-Sud, 91405 Orsay Cedex (France)

[d] A. Pinto
Department of Organic Chemistry, University of Geneva
30 quai E. Ansermet, 1211 Geneva 4 (Switzerland)

Supporting information for this article is available on the WWW under http://www.chemeurj.org/ or from the author.

WILEY InterScience DISCOVER SOMETHING GREAT
© 2007 Wiley-VCH Verlag GmbH & Co. KGaA, Weinheim

spired chemistry, especially because the Mo^{V} oxo or thio species are involved as active sites in many metalloenzymes, mainly for oxygen-transfer reactions.[30,31] In a related work, we are systematically investigating the self-assembling properties of the hexaaquo $[Mo_2O_2S_2(OH_2)_6]^{2+}$ ion in the presence of specific templates. However, the design of cyclic molecular materials with controlled ring-size and deliberate properties requires additional knowledge about the driving forces governing the formation and stability of the host–guest assembly. Linear saturated dicarboxylate ions with various lengths of the alkyl chain (from C2 to C8) gave highly flexible and fluxional host–guest architectures with nuclearity varying in the Mo8–Mo12 range.[28,32] These results highlight a mutual adaptability and concerted dynamics between the host and guest. The use of rigid templates (unsaturated[27] or aromatic polycarboxylate ions[29]) is expected to bring rigidity to the host–guest system. In addition, the targeted stereochemistry of the template (position of the anchoring carboxylate groups or presence of bulky groups), supported by the physical properties (hydrophobic area, π system), is expected to produce a spectacular extension of the nuclearity through subtle weak intramolecular interactions.

In the present study, we report three new host–guest systems involving rigid or semi-rigid terephtalate derivatives: terephtalate (denoted $TerP^{2-}$), isophtalate ($IsoP^{2-}$), and phenylenediacetate (PDA^{2-}) ions (see Scheme 1). These ligands lead to twelve- or sixteen-membered rings that are fully characterized both in the solid state and in solution by extensive NMR studies. Importantly, ^{1}H diffusion-ordered spectroscopy, DOSY, is used to characterize the speciation of cyclic polyoxothiomolybdates in solution. Finally, the dynamic and thermodynamic properties of the new hexadecamolybdenum wheels, $[Mo_{16}(IsoP)_2]^{4-}$ and $[Mo_{16}(PDA)_2]^{4-}$, were deduced and discussed in relationship with weak intramolecular interactions occurring between the inner guest moieties.

Results and Discussion

Structures of the anions: The molecular structures of $[Mo_{12}TerP]^{2-}$, $[Mo_{16}(PDA)_2]^{4-}$, and $[Mo_{16}(IsoP)_2]^{4-}$ are depicted in Figures 1 and 2. Crystal data are given in Table 1, whereas selected bond lengths and angles are listed in Tables S1 and S2 in the Supporting Information. The three molecular architectures consist of a cyclic inorganic neutral skeleton $[Mo_{2n}S_{2n}O_{2n}(OH)_{2n}]$, with $n=6$ or 8, encapsulating one or two guest dicarboxylate anions, respectively. The inorganic architectures result from connections between the $[Mo_2S_2O_2]^{2+}$ building blocks by double hydroxo bridges. Short Mo–Mo distances within the dinuclear units

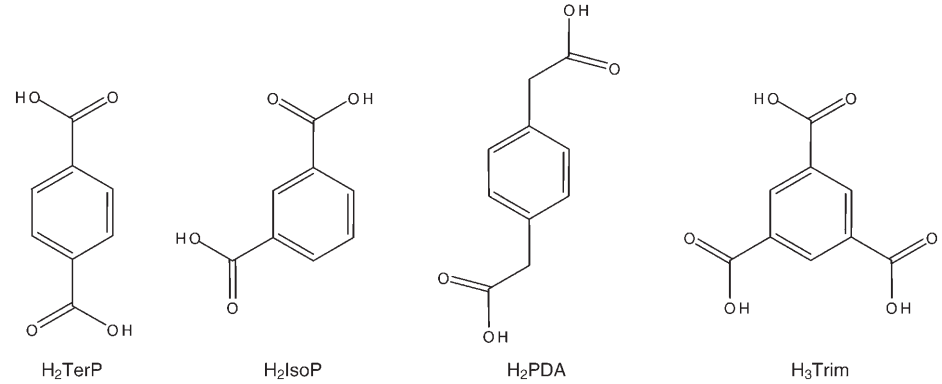

Scheme 1. Drawing of carboxylate ligands used in the present study.

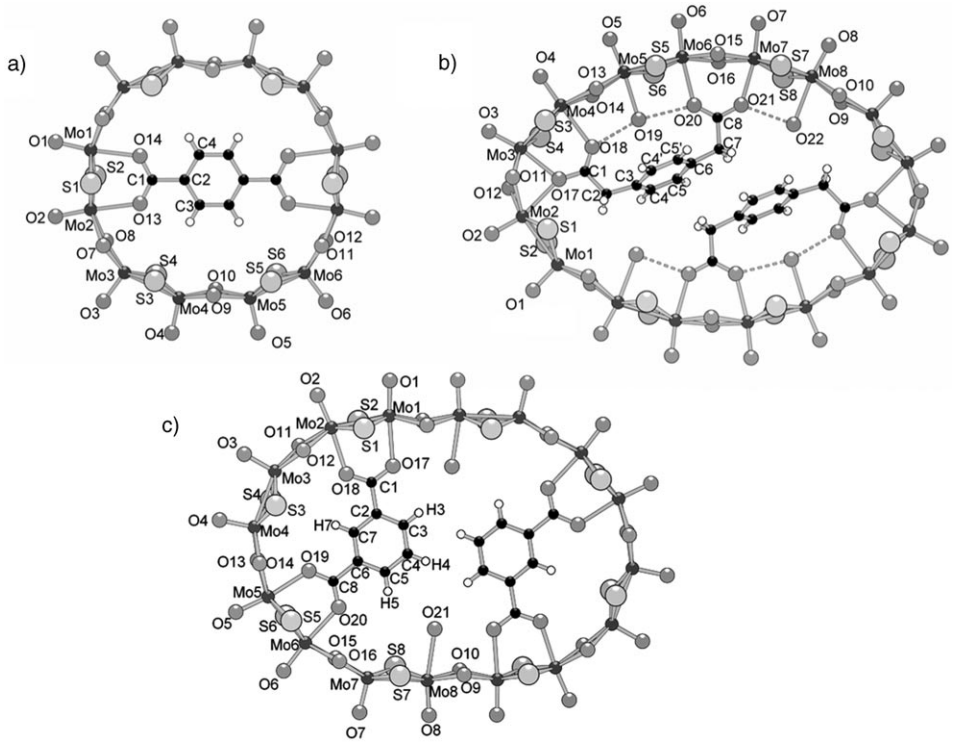

Figure 1. Labeled molecular structure of the complexes $[Mo_{12}TerP]^{2-}$ (a), $[Mo_{16}(PDA)_2]^{4-}$ (b), and $[Mo_{16}(IsoP)_2]^{4-}$ (c).

 © 2007 Wiley-VCH Verlag GmbH & Co. KGaA, Weinheim

Table 1. Structural parameters for compounds $Cs_2[Mo_{12}TerP]$, $Cs_4[Mo_{16}(PDA)_2]$, and $(NMe_4)_4[Mo_{16}(IsoP)_2]$.

Compound	$Cs_2[Mo_{12}TerP]$	$Cs_4[Mo_{16}(PDA)_2]$	$(NMe_4)_4[Mo_{16}(IsoP)_2]$
empirical formula	$Cs_2Mo_{12}S_{12}O_{42}C_{44}N_{12}H_{104}$	$Cs_4Mo_{16}S_{16}O_{74}C_{20}H_{100}$	$N_4Mo_{16}S_{16}O_{67.50}C_{32}H_{127}$
formula weight [g mol^{-1}]	3275.21	4104.64	3696.38
temperature [K]	296(2)	293(2)	296(2)
wavelength [Å]	0.71073	0.71073	0.71073
crystal size [mm]	$0.14\times0.12\times0.08$	$0.30\times0.20\times0.15$	$0.34\times0.14\times0.10$
crystal system	triclinic	monoclinic	triclinic
space group	$P\bar{1}$	$P2(1)/c$	$P\bar{1}$
a [Å]	10.4492(9)	17.528(2)	12.1908(3)
b [Å]	17.2000(14)	19.940(2)	13.6273(5)
c [Å]	18.2021(13)	18.253(2)	20.9504(7)
α [°]	63.198(3)	90	82.8740(10)
β [°]	84.719(3)	112.795(5)	83.5080(10)
γ [°]	78.883(4)	90	64.5800(10)
V [Å^3]	2865.1(4)	5881.4(11)	3112.25(17)
Z	1	2	1
ρ_{calcd} [g cm^{-3}]	1.898	2.318	1.972
μ [mm^{-1}]	2.182	3.235	1.903
θ range for data collection	1.25 to 30.18°	1.26 to 30.08°	0.98 to 30.06°
F(000)	1594	3920	1815
limiting indices	$-14\le h\le14$ $-24\le k\le24$ $-25\le\ \le23$	$-24\le h\le24$ $-27\le k\le28$ $-25\le\ \le22$	$-14\le h\le17$ $-18\le k\le19$ $-29\le\ \le29$
completeness to θ_{max} [%]	98.9	99.5	99.5
data/restraints/parameters	16817/0/571	17183/0/637	18176/0/667
R(int)	0.0312	0.0666	0.0317
GOF on F^2	1.066	1.085	1.160
final R indices [$I>2\sigma(I)$]			
$R1$	0.0332	0.0590	0.0345
$wR2$	0.0963	0.1387	0.1050
largest diff peak and hole [e A^{-3}]	1.428 and −0.741	2.069 and −2.263	1.321 and −0.787

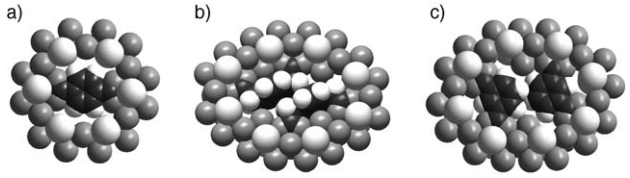

Figure 2. Space-filling model of the complexes $[Mo_{12}TerP]^{2-}$ (a), $[Mo_{16}(PDA)_2]^{4-}$ (b), and $[Mo_{16}(IsoP)_2]^{4-}$ (c).

(2.800(1)–2.849(1) Å) characteristic of metal–metal bonds alternate with long Mo–Mo interblock distances which span nonbonding contacts (3.279(1)–3.410(1) Å).

$[Mo_{12}O_{12}S_{12}(OH)_{12}(C_8H_4O_4)]^{2-}$, $[Mo_{12}TerP]^{2-}$: The dodecamolybdenum wheel $[Mo_{12}TerP]^{2-}$ consists of six $[Mo_2S_2O_2]^{2+}$ fragments assembled around a terephtalate ligand (Figures 1a and 2a). The $[Mo_{12}TerP]^{2-}$ ion retains an idealized D_{2h} symmetry, mainly imposed by the rigid $TerP^{2-}$ ion. The two symmetric carboxylate groups bridge the Mo1 and Mo2 atoms of the same $[Mo_2S_2O_2]^{2+}$ moiety through single Mo–O interactions (d[Mo2–O13] 2.351(2) Å and d[Mo1–O14] 2.329(2) Å). Consequently, the Mo1 and Mo2 atoms retain an octahedral environment, whereas the eight remaining Mo atoms (Mo3–Mo6) display square-pyramidal arrangements. For steric constraints and/or unfavorable hydrophobic interactions induced by the presence of the $TerP^{2-}$ ion, no inner coordinated water was found in the axial position, *trans* to the Mo=O double bonds. The space-filling representation of the anion (Figure 2a) highlights the close compact host–guest arrangement, with no available inner space within the cyclic molecule.

$[Mo_{16}O_{16}S_{16}(OH)_{16}(H_2O)_4(C_{10}H_8O_4)_2]^{4-}$, $[Mo_{16}(PDA)_2]^{4-}$: The cyclic arrangement of $[Mo_{16}(PDA)_2]^{4-}$ exhibits a "rugby-ball shape" and retains the C_{2h} nominal symmetry in the solid state (Figures 1b and 2b). The inner cavity contains two equivalent PDA^{2-} ions, arranged as a pillar within the molecule and four terminal aquo ligands, distributed as two equivalent pairs (O19 and O22). The two equivalent PDA^{2-} ions are asymmetrically bound to the inorganic host. One carboxylate group (O20-C8-021) exhibits two singly bound oxygen atoms, O20 and O21, connected to the adjacent Mo6 and Mo7, with Mo–O distances of 2.356(4) and 2.286(1) Å, respectively. The opposite carboxylate group O17-C1-O18 is asymmetrically coordinated with a singly bound oxygen atom O18 (Mo4···O18 2.465(5) Å), whereas the O17 atom bridges Mo2 and Mo3 with Mo3···O17 2.498(5) and Mo2···O17 2.329(6) Å. The four terminal inner water molecules, O19 and O22, are bound to the Mo5 and Mo8 atoms through usual bond lengths of 2.330(6) and 2.423(6), respectively. As suggested by the O···O distances in the (2.648(8)–2.705(8) Å) range, these water molecules interact with the neighboring carboxylate groups through hydrogen bonds. The O19 water molecule exhibits a remarkable environment and appears to be closely located in a pocket lined by the Mo4-Mo5-Mo6 atoms of the inorganic ring and the PDA^{2-} anion. Both the water molecules cap the aromatic cycle through quite short O···C distances in the

 © 2007 Wiley-VCH Verlag GmbH & Co. KGaA, Weinheim

(3.290(11)–3.336(9) Å) narrow range. The aromatic cycles within PDA^{2-} are perpendicularly positioned with respect to the host ring, but both aromatic cycles are parallel and significantly staggered by about 3.8 Å through a gliding surface. The short separation between both the aromatic cycles, especially between the two C6 atoms (3.522(10) Å), suggests weak π–π stacking interactions (see Figure 3). The two

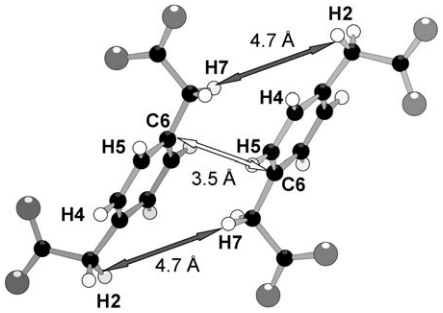

Figure 3. Interactions between the two ligands PDA^{2-} in $[Mo_{16}(PDA)_2]^{4-}$. The grey double arrows indicate the intermolecular NOE effect between H1 and H4 protons whereas the white double arrow indicates the π–π stacking between C6 carbon atoms.

equivalent Mo1 atoms display square-pyramidal environments because no water molecule was found *trans* to the Mo1=O1 double bond. Finally, the space-filling sketch (Figure 2b) shows the close arrangement of the inner components of the wheel, which mutually interact through weak hydrogen-bonding and π–π stacking interactions.

$[Mo_{16}O_{16}S_{16}(OH)_{16}(H_2O)_2(C_8H_4O_4)_2]^{4-}$, $[Mo_{16}(IsoP)_2]^{4-}$: The Mo_{16} ring contains two $IsoP^{2-}$ ions which are conventionally anchored to the inorganic moiety through the carboxylate groups, which bridge two adjacent molybdenum atoms through single bonds Mo–O in the usual range of distances (2.296(2)–2.383(2) Å, see Figure 1c). The anionic ring displays lowered C_i symmetry in the solid state (compared to C_{2h} for $[Mo_{16}(PDA)_2]^{4-}$) because the two equivalent aromatic cycles are not contained in the plane of the host ring. Each aromatic ring is significantly displaced by about 11.5(8)° from the plane defined by the sixteen Mo atoms. Both aromatic cycles are parallel and then mutually arranged in an *anti* conformation. Such an arrangement is likely to be imposed by steric constraints, due to the inner bulky aromatic groups (see space-filling sketch of $[Mo_{16}(IsoP)_2]^{4-}$ in Figure 2c), which are mutually interdigitated through hydrophobic interactions. The shortest intercycle C···C separation is 3.693(5) Å. Two terminal inner aquo ligands, labeled O21 are attached to the Mo8 atoms, whereas six Mo atoms, denoted as Mo3, Mo4, and Mo7 display square-pyramidal environments. Moderate internal hydrogen bonds between the terminal aquo ligand O21 and the oxygen atom O17 belonging to the adjacent carboxylate group are observed with a characteristic O···O distance of 2.829(3) Å.

NMR studies in solution: Diffusion NMR methods offer a powerful tool to characterize dynamic entities in solution and were successfully applied for the characterization of biological or supramolecular systems in solution, such as, proteins, ion pairs[33], or polymetallic coordination complexes.[34–36] In this context, we applied the DOSY NMR technique to determine the nuclearity of the host–guest systems based on the anions $[Mo_{12}TerP]^{2-}$, $[Mo_{16}(PDA)_2]^{4-}$, and $[Mo_{16}(IsoP)_2]^{4-}$ in solution. Assuming that the Einstein–Smoluchowski–Stokes auto-diffusion theory holds, the auto-diffusion coefficient D_x of a given compound x in solution is proportional to the quantity $(\tilde{\nu}_x \cdot MM_x)^{-1/3}$, whereby MM_x stands for the molecular weight and $\tilde{\nu}_x$ corresponds to the specific partial volume.[37] The diffusion coefficients D_x of our three compounds were measured with respect to that of $[Mo_{12}Trim]^{3-}$ ion[29] ($MM_r = 2139\ g\,mol^{-1}$), used as an internal suitable reference. Indeed, the $[Mo_{12}Trim]^{3-}$ ion retains a similar cyclic arrangement ($\tilde{\nu}_r \approx \tilde{\nu}_x$), appears highly stable in any solvent (D_2O, DMSO), undergoes no chemical exchange with other species, and exhibits a single sharp resonance for the encapsulated ligand (see Figure S1 in the Supporting Information) which does not overlap with the signals of $[Mo_{12}TerP]^{2-}$, $[Mo_{16}(PDA)_2]^{4-}$, and $[Mo_{16}(IsoP)_2]^{4-}$. In these conditions, the D_r/D_x ratio is equal to the cubic root of the ratio MM_x/MM_r [Eq. (1)],[37] which leads easily to the unknown MM_x value.

$$\frac{D_r}{D_x} = \sqrt[3]{\frac{MM_x}{MM_r}} \qquad (1)$$

Figure 4 shows the decay of the natural logarithm of the normalized signal intensity I/I_0 of a selected signal of the aromatic rings of guests in $[Mo_{12}TerP]^{2-}$, $[Mo_{16}(PDA)_2]^{4-}$, and $[Mo_{16}(IsoP)_2]^{4-}$, and that of the $[Mo_{12}Trim]^{3-}$ as a function of the square of the pulse gradient strength. The diffusion coefficient D_x was extracted from the slope of the regression line $\ln(I/I_0)$ versus G^2, according to Equation (2)[33] (I is the observed intensity, I_0 is the intensity without gradients, γ is the gyromagnetic ratio of the observed nucleus, δ is the length of the gradient pulse, G is the gradient strength, Δ

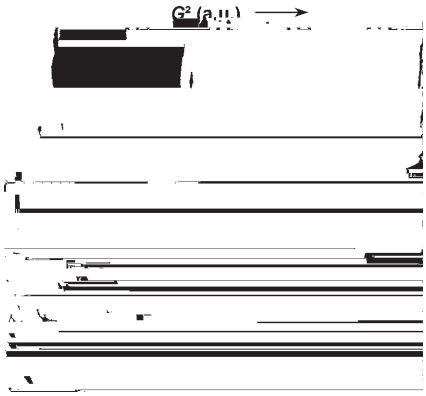

Figure 4. Variation of $\mathrm{Ln}(I/I_0)$ plot as a function of G^2 for $[Mo_{12}\text{-}TerP]^{2-}$ (△), $[Mo_{12}Trim]^{3-}$ (●), $[Mo_{16}(PDA)_2]^{4-}$ (▲), and $[Mo_{16}(IsoP)_2]^{4-}$ (□).

 © 2007 Wiley-VCH Verlag GmbH & Co. KGaA, Weinheim

(diffusion delay) is the delay between the midpoints of the gradients).

$$\ln\left(\frac{I}{I_0}\right) = -(\gamma\delta)^2\left(\Delta-\frac{\delta}{3}\right)DG^2 \qquad (2)$$

$[Mo_{12}TerP]^{2-}$ ion: The ^{1}H NMR spectrum of $Cs_2[Mo_{12}TerP]$ was recorded in [D$_6$]DMSO and in D$_2$O (see Figures 5 and S2 in the Supporting Information). In [D$_6$]DMSO, the spectrum of $[Mo_{12}TerP]^{2-}$ displays three sharp resonances at $\delta =$ 5.07, 10.58, and 11.45 ppm with an integration of 1:2:1, respectively. The low frequency signal at $\delta = 5.07$ ppm corresponds to the four aromatic protons of the encapsulated $TerP^{2-}$ guest, which appears significantly shielded by about 2.77 ppm with respect to the free $TerP^{2-}$ ion ($\delta = 7.84$ ppm). Such a shielding for the encapsulated guest within $\{Mo_{2n}\}$ rings corresponds to a general feature, but has been observed in several systems containing polycarboxylate or mono- and polyphosphate ions.[21–23,28,29] Magnetic anisotropy arising from the inorganic ring is probably responsible for such a general shielding effect. The deshielded resonances at $\delta = 11.45$ and 10.58 ppm are attributed to the hydroxo bridges in a D_{2h}-idealized symmetry. On the basis of its integration, the single resonance at $\delta = 10.48$ ppm corresponds to the eight protons attached to the equivalent oxygen atoms, labeled O7, O8, O11, and O12 in the crystallographic model. The $\delta = 11.45$ ppm line corresponds to the four remaining equivalent protons linked to the O9 and O10 oxygen atoms. An additional signal, at about $\delta = 8$ ppm corresponds to the DMF formamide proton, present as solvate in the crystals of $Cs_2[Mo_{12}TerP]$. The sharpness of the resonances of the inorganic and organic protons of the anion $[Mo_{12}TerP]^{2-}$, compared to those arising from host–guest systems containing flexible linear carboxylate ions[28] is related to the rigidity of the central $TerP^{2-}$ ion, which prevents any observable dynamics on the NMR time scale. In D$_2$O (see Figure S2 in the Supporting Information), the resonances related to the hydroxo bridges disappeared because fast proton–deuterium exchanges occur in aqueous solvent. The resonance of the four aromatic protons of the encapsulated $TerP^{2-}$ ion are observed at $\delta = 5.18$ ppm, whereas about six DMF molecules as solvate are evidenced by the resonance at $\delta = 7.75$ ppm.

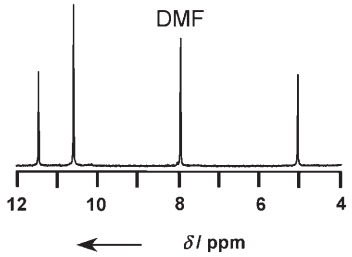

Figure 5. 300 MHz ^{1}H NMR spectrum of $[Mo_{12}TerP]^{2-}$ in [D$_6$]DMSO.

The chemical shift of ligands and complexes, D_r/D_x ratios, and the calculated molecular weights are summarized in Table 2. In DMSO and D$_2$O solution, the DOSY experiments give $D_r/D_x = 0.96$ and 0.97 respectively, which are fully consistent with the very close molecular weight of the $[Mo_{12}Trim]^{3-}$ ion ($MM_r = 2139$ g mol^{-1}) and the $[Mo_{12}TerP]^{2-}$ ion ($MM_x = 2096$ g mol^{-1}), calculated from the solid-state structure. In conclusion, these results demonstrate that the DOSY 1D NMR technique is a reliable method, providing specific additional data about these systems in solution.

Table 2. ^{1}H NMR chemical shifts of free or coordinated ligands, and D_r/D_x ratio and molecular weights obtained with DOSY NMR. Calculated values are given in parentheses.

Compound	Solvent	δ [ppm] (Multiplicity)	D_r/D_x found (calcd)	MM_x found [g mol^{-1}] (calcd)
$Trim^{3-}$	D$_2$O	8.28(s)	–	–
$[Mo_{12}Trim]^{3-}$	D$_2$O	5.92(s)	–	2139
$[Mo_{12}Trim]^{3-}$	[D$_6$]DMSO	10.04(s); 5.93(s)	–	2139
$TerP^{2-}$	D$_2$O	7.84(s)	–	–
$[Mo_{12}TerP]^{2-}$	D$_2$O	5.18(s)	0.97 (0.99)[a]	1950 (2096)
$[Mo_{12}TerP]^{2-}$	[D$_6$]DMSO	11.45(s); 10.58(s); 5.07(s)	0.96 (0.99)[a]	1910 (2096)
PDA^{2-}	D$_2$O	7.19(s); 3.49(s)	–	–
$[Mo_{16}(PDA)_2]^{4-}$	D$_2$O	0.70(s); 1.58(s); 5.69(d); 5.85(d)	1.17 (1.12)[a]	3430 (3032)
$IsoP^{2-}$	D$_2$O	8.17(s); 7.86(d); 7.40(t)	–	–
$[Mo_{16}(IsoP)_2]^{4-}$	D$_2$O	6.45(d); 6.20(t); 6.14(s)	1.14 (1.12)[a]	3180 (2997)
$[Mo_{12}\text{-}IsoP]^{2-}$	D$_2$O	5.70(s); 5.39(d); 4.82(t)	0.92 (0.99)[b]	2260 (2096)

[a] $[Mo_{12}Trim]^{3-}$ used as an internal reference. [b] $[Mo_{16}(IsoP)_2]^{4-}$ ion used as an internal reference.

$[Mo_{16}(PDA)_2]^{4-}$ ion: The ^{1}H NMR spectrum of $Rb_4[Mo_{16}(PDA)_2]$ in D$_2$O (see Figure 6) consists of four equal signals,

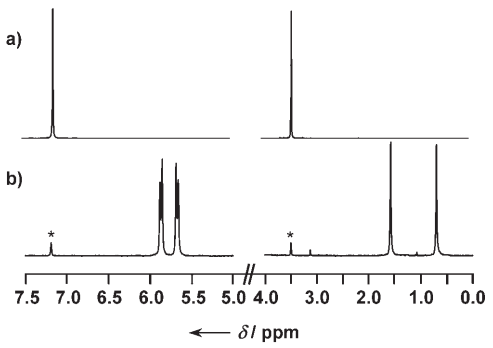

Figure 6. 300 MHz ^{1}H NMR spectra in D$_2$O of ligand PDA^{2-} (a); and $[Mo_{16}(PDA)_2]^{4-}$ (b) in D$_2$O; * indicates a small amount of free ligand as minor impurity.

© 2007 Wiley-VCH Verlag GmbH & Co. KGaA, Weinheim

distributed as two single resonances at $\delta = 1.58$ and 0.70 ppm and two doublets of equal intensity centered at $\delta = 5.85$ and 5.69 ppm ($J = 8$ Hz for both, respectively), which correspond to a frozen conformation for the PDA^{2-} ion with a local C_s symmetry. In contrast, the free ligand (D_{2h}-averaged symmetry) exhibits only two equal single resonances at $\delta = 7.19$ and 3.49 ppm assigned to the aromatic protons and the methylene protons. The $\{^1H,^1H\}$ COSY two-dimensional (2D) spectrum (not shown) confirms the scalar coupling between the aromatic proton H4 (H4′) and H5 (H5′). The expected shielding on the ^1H nuclei due to the encapsulation of the PDA^{2-} is also observed. The mean value for the chemical shift shielding is about $\delta = -1.42$ ppm for the aromatic proton, and $\delta = -2.35$ ppm for the methylene groups. The NOESY 2D spectrum recorded in D_2O (not shown) exhibits NOE correlations between all the possible protons pairs labeled H2–H4, H2–H5, H2–H7, H4–H5, H4–H7, and H5–H7 (see Figure 3). The dipolar coupling between H2–H4 and H2–H5 results from intramolecular interactions (2.4–4.5 Å). For H5–H7, H4–H5, and H4–H7 pairs, the dipolar interactions arise from conjugated intra and intermolecular contributions ($dH–H_{intra} = 2.3–4.5$ Å; $dH–H_{inter} = 3.2–5.0$ Å). The H2–H7 NOE correlation (between both the distinguishable methylene groups) can be unambiguously attributed to intermolecular dipolar coupling between the two close PDA^{2-} ligands ($dH2–H7_{inter} = 4.7$; $dH2–H7_{intra} = 6.5$ Å). Such a result evidences the close arrangement between the two ligands PDA^{2-} inside the molybdenum wheel, according to the structure of $[Mo_{16}(PDA)_2]^{4-}$ in the solid state. The ^{13}C NMR spectrum of the highly soluble lithium salt of $[Mo_{16}(PDA)_2]^{4-}$ in D_2O (see Figure S3 in the Supporting Information) exhibits eight well-resolved peaks at $\delta = 176.3$, 175.4 ppm corresponding to the carboxylate groups, at $\delta = 132.8$, 132.6, 130.0, 129.6 ppm for the aromatic carbons, and at $\delta = 41.5$ and 40.4 ppm for the methylene carbon atoms. Such a ^{13}C NMR feature is still fully consistent with an anchored PDA^{2-} in a C_s frozen conformation. In contrast, the free ligand (D_{2h} averaged symmetry) gives four peaks at $\delta = 181.2$, 135.2, 129.2, and 44.0 ppm. The encapsulated carbon atoms are shielded by about 6 ppm for the carboxylates, 3–4 ppm for the methylene, whereas the aromatic carbons are deshielded by 0–3 ppm. Interestingly, $[Mo_{16}(PDA)_2]^{4-}$, in contrast to $[Mo_{12}TerP]^{2-}$, appears unstable in DMSO and decomposes into smaller molybdenum fragments (see Figure S4 in the Supporting Information).

The rubidium salt of $[Mo_{16}(PDA)_2]^{4-}$ was studied by DOSY NMR spectroscopy in D_2O (see Figure 4 and Table 2). An experimental D_r/D_x ratio of 0.85 was found with $r = [Mo_{12}Trim]^{3-}$. The calculated experimental molecular weight for $[Mo_{16}(PDA)_2]^{4-}$ is $MM_x = 3430\ g\,mol^{-1}$ and appears slightly larger than the expected one, calculated from the X-ray data ($3032\ g\,mol^{-1}$). The origins of this discrepancy could mainly arise from the several approximations required to obtain the Equation (1) and hydration effects. Indeed, the model is built for the isotropic spherical molecule[37,38] and the specific partial volumes of the reference and of the studied samples are considered as strictly equal ($\tilde{\nu}_r \approx \tilde{\nu}_x$), whereas the compounds r and x retain different sizes and shapes. Moreover, the solvation spheres of the compounds x and r are not taken into account in the present study and should be also considered to improve the accuracy of this technique. Especially, in this paper, r and x molecules retain different charges, and then probably a different number of solvates in solution. Further investigations on this point are currently in progress.

The ^1H NMR study in D_2O (see Figure S5 in the Supporting Information) recorded upon varying the ratio between the cyclic precursor $K_{2-x}(NMe_4)_x[I_2Mo_{10}O_{10}S_{10}(OH)_{10}(H_2O)_5]$ and the PDA^{2-} ion reveals that the single species $[Mo_{16}(PDA)_2]^{4-}$ is exclusively formed whatever the ratio of the reactants. This study shows that the formation of $[Mo_{16}(PDA)_2]^{4-}$ is quantitative and fast (a few minutes to reach the equilibrium state at room temperature).

The variable-temperature ^1H NMR spectra of $[Mo_{16}(PDA)_2]^{4-}$ in D_2O are shown in Figure 7. As the temperature increases, the signals of the aromatic and methylene protons broaden gradually. The coupling pattern between the aromatic protons first vanishes, then both the resonances assigned to the aromatic protons collapse to give a broad signal at $T = 345$ K which then sharpens until $T = 360$ K. Concomitantly, the signals of the methylene protons observed at $\delta = +0.70$ and $+1.58$ ppm for $T = 300$ K exhibit the same behavior and collapse at 360 K. Such a result reveals a dynamic molecular process in solution, which increases the observed symmetry of the anchored PDA^{2-} ion from C_s to an averaged local C_{2v} symmetry. A simple and reasonable dynamic mechanism can be postulated, corresponding to the gliding of the parallel aromatic cycles. As depicted in Scheme 2, this rapid conformational change can be viewed as a "flip-flop" motion, which takes place between two equivalent C_{2h} conformations established in the solid state. From the coalescence temperature (T_c) of the aromatic, or of the methylene protons ($T_c = 345$ K and 360 K,

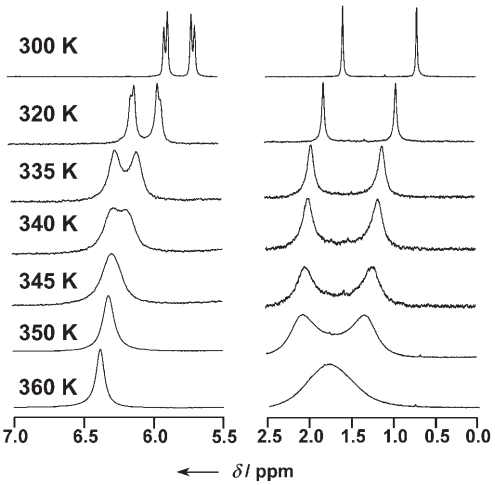

Figure 7. Variable-temperature 300 MHz ^1H NMR spectra of $[Mo_{16}(PDA)_2]^{4-}$ in D_2O.

 © 2007 Wiley-VCH Verlag GmbH & Co. KGaA, Weinheim

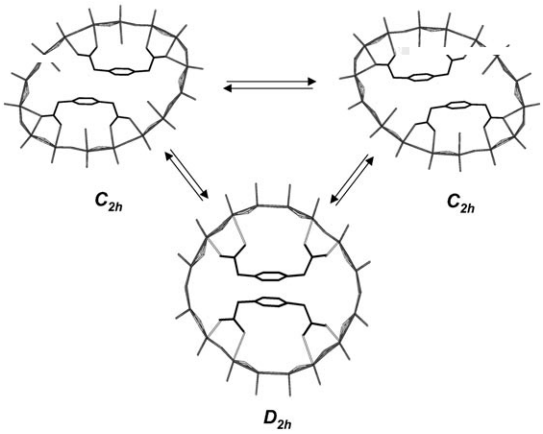

Scheme 2. Postulated dynamic equilibrium between the two equivalent C_{2h} limit conformations of $[Mo_{16}(PDA)_2]^{4-}$ in solution.

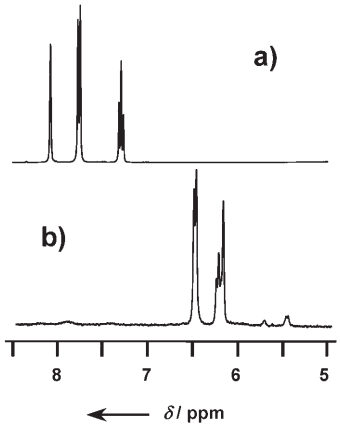

Figure 8. 300 MHz ^{1}H NMR spectra in D_2O of ligand $IsoP^{2-}$ (a); and complex $[Mo_{16}(IsoP)_2]^{4-}$ (b).

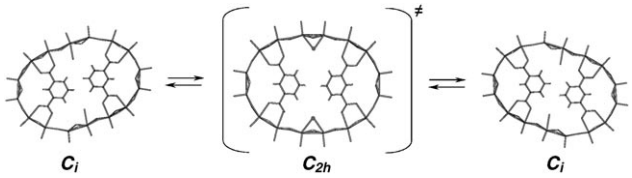

Scheme 3. Dynamical equilibrium between the two equivalent C_i limit conformations of $[Mo_{16}(IsoP)_2]^{4-}$ in solution.

respectively), calculations by using the Eyring model [Eq. (3) and (4)], [39] give an estimation for the free activation energy $\Delta G^{\neq}$, where T_c is the coalescence temperature, $\Delta\nu$ is the frequency difference at 300 K under no-exchange conditions (60 and 264 Hz for the aromatic protons and the methylene groups, respectively), R, k_b and h are the molar gas constant, the Boltzman and Planck constants, respectively.

$$\Delta G^{\neq} = RT_c \ln\left(\frac{k_b T_c}{kh}\right) \quad (3)$$

$$k = \frac{\pi\Delta\nu}{\sqrt{2}} \quad (4)$$

The calculated $\Delta G^{\neq} = (70 \pm 1)\,kJ\,mol^{-1}$ is a large value mainly due to: 1) the rigidity of the inner PDA^{2-} ion; 2) the close compact arrangement within the ring and; 3) the network of weak intramolecular interactions (hydrogen bonds and π–π stacking).

$[Mo_{16}(IsoP)_2]^{4-}$ ion: The ^{1}H NMR of the $[Mo_{16}(IsoP)_2]^{4-}$ in D_2O exhibits a doublet centered at $\delta = 6.45$ ppm, a triplet at $\delta = 6.20$ ppm, and a singlet at $\delta = 6.14$ ppm in a 2:1:1 intensity ratio (see Figure 8). This ^{1}H NMR pattern, similar to that of the free $IsoP^{2-}$ ligand agrees with a local C_{2v} symmetry for the anchored ligand. In solution, the H3 and H5 protons become equivalent. The triplet corresponds to the H4 proton, coupled with the equivalent H3–H5 protons ($J =$ 8 Hz), the doublet is assigned to the equivalent H3–H5 proton coupled to H4 and the singlet is attributed to the isolated H7 proton. Through encapsulation, the chemical shifts are shielded ($\Delta\delta = -1.20$ ppm for the triplet, -1.41 ppm for the doublet, and -2.03 ppm for the singlet). The increased symmetry of $[Mo_{16}(IsoP)_2]^{4-}$ on going from the solid state to the solution is related to a rapid process occurring at room temperature and resulting from the swinging of both the aromatic cycles between the two equivalent *Ci* conformations (Figure 1c and Scheme 3). An identical conclusion is obtained from the ^{13}C NMR spectrum recorded in D_2O (see Figure S6 in the Supporting Information), for which only four NMR lines are obtained, compared to the eight expected from the solid state. This process exhibits a weak temperature dependence because in the 273–350 K range, the line widths of the three resonances do not vary significantly, likely due to a low $\Delta G^{\neq}$ activation parameter for such a process. These results could originate from: 1) the weak amplitude of the swinging angle between both limiting conformations (about 20°); 2) the weak hydrophobic interactions between the aromatic cycle and; 3) the labile inner water molecule, labeled O21, easily exchangeable between the two adjacent coordination sites, Mo8 and Mo7.

DOSY NMR experiments give the experimental ratio $D_r/D_x = 0.88$, which leads to a molecular weight of 3180 g mol^{-1}. These data evidence the existence of the $[Mo_{16}(IsoP)_2]^{4-}$ ion ($M = 2997$ g mol^{-1}) in D_2O, but in DMSO, the $[Mo_{16}(IsoP)_2]^{4-}$ anion decomposes into several unidentified species (see Figure S7 in the Supporting Information).

The variable-temperature ^{1}H NMR spectra of $[Mo_{16}(IsoP)_2]^{4-}$ were recorded in D_2O and are shown in Figure 9. When the temperature increases, the signals of $[Mo_{16}(IsoP)_2]^{4-}$ broaden and the triplet and the singlet assigned to H4 and H7 protons at 300 K overlap to give broad signals and are significantly deshielded by about 0.4–0.5 ppm. Besides, as the temperature increases, additional resonances gradually appear as two sets of three lines with 1:2:1 integrations. The deshielded three broad peaks centred around 8.75, 8.45 and 7.90 ppm, respectively, are confidently attributed to the uncoordinated $IsoP^{2-}$ ion, but the three other shielded peaks at $\delta = 5.70$ (singlet), 5.39 (doublet), and 4.82 ppm (triplet) correspond to a novel $IsoP^{2-}$ containing cyclic architecture, with a C_{2h} or a D_{2h} symmetry. This equilibrium is reversible but kinetically slow (about several

 © 2007 Wiley-VCH Verlag GmbH & Co. KGaA, Weinheim

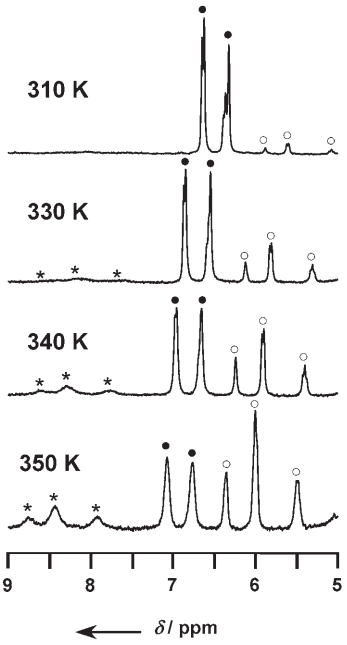

Figure 9. Variable-temperature 300 MHz ^{1}H NMR spectra of $[Mo_{16}(IsoP)_2]^{4-}$ in D_2O. (●) $[Mo_{16}(IsoP)_2]^{4-}$; (○) $[Mo_{12}IsoP]^{2-}$; (*) free ligand $IsoP^{2-}$.

hours), which enables DOSY measurements to be performed on the latter. By using $[Mo_{16}(IsoP)_2]^{4-}$ as an internal reference, DOSY NMR gives $D_r/D_x = 0.92$, which translates into $MM_x = 2260\ g\,mol^{-1}$, a value in good agreement with the formula $[Mo_{12}O_{12}S_{12}(OH)_{12}(IsoP)]^{2-}$ (2096 g mol^{-1}). From this result, the equilibrium shown in (5) can be postulated.

$$3\,[Mo_{16}(IsoP)_2]^{4-} \rightleftharpoons 4\,[Mo_{12}IsoP]^{2-} + 2\,IsoP^{2-} \quad (5)$$

The distribution of the three components in solution as a function of temperature is given in Figure 10. The increase of the quantity of free ligand is half that of the new previous molybdenum complex, which confirms equilibrium (5). Calculation of K_{eq} for each temperature in the 310–350 K range, followed by a Van't Hoff treatment (see insert in Figure 10), allows the estimation of $\Delta_r H^* = +273\ kJ\,mol^{-1}$ and $\Delta_r S^* = +658\ J\,mol^{-1}\,K^{-1}$.

Conclusion

Three new molybdenum rings have been discovered and studied in both the solid state and in solution, with three terephtalate derivatives. A highly symmetrical dodecamolybdenum wheel, namely $[Mo_{12}O_{12}S_{12}(OH)_{12}(TerP)]^{2-}$ ($[Mo_{12}TerP]^{2-}$), was obtained with a terephtalate guest, whereas two large hexadecanuclear inorganic rings were self-assembled around two $IsoP^{2-}$ or two PDA^{2-} ligands: $[Mo_{16}O_{16}S_{16}(OH)_{16}(H_2O)_4(PDA)_2]^{4-}$ ($[Mo_{16}(PDA)_2]^{4-}$) and $[Mo_{16}O_{16}S_{16}(OH)_{16}(H_2O)_2(IsoP)_2]^{4-}$ ($[Mo_{16}(IsoP)_2]^{4-}$), respectively. The two latter wheels are the largest molybdenum wheels obtained by using internal pillar ligands and were fully characterized by combining X-ray studies and various NMR techniques. Especially, the DOSY NMR method has been validated with $[Mo_{12}TerP]^{2-}$ compound, and was then widely used in this paper for identifying molybdenum complexes in solution. This method, used as a routine technique by using standard apparatus, NMR tubes, and processing packages, allows a molecular weight determination with about 10% accuracy and allows a wide application of this method in number of laboratories.

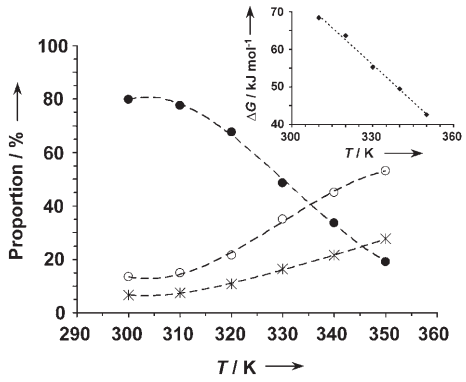

Figure 10. Speciation in solution diagram as a function of temperature. (●) $[Mo_{16}(IsoP)_2]^{4-}$; (○) $[Mo_{12}IsoP]^{2-}$; (*) free ligand $IsoP^{2-}$. Dotted lines are only guides for eyes. Insert: Variation of $\Delta_r G^{\neq}$ as a function of temperature.

Investigations of the sixteen-membered rings reveal very contrasting properties in solution between $[Mo_{16}(PDA)_2]^{4-}$ and $[Mo_{16}(IsoP)_2]^{4-}$. $[Mo_{16}(PDA)_2]^{4-}$ appears stable and highly fluxional, the latter exhibiting dynamic behavior consistent with the gliding of both the stacked aromatic groups. Conversely, $[Mo_{16}(IsoP)_2]^{4-}$ is labile and gives rise to a temperature-dependent equilibrium process with the mono-templated complex $[Mo_{12}\text{-}IsoP]^{2-}$.

This study provides a better understanding of the self-assembly of large molybdenum wheels around polycarboxylate ligands and constitutes an important step towards the controlled design of functional cyclic molecular polyoxothiomolybdate through the programming of the templates, and the control of intermolecular π–π, hydrophobic and/or hydrogen-bond interactions. These key parameters are at the origin of the driving forces governing the formation and stability of large host–guest assemblies.

Experimental Section

Physical methods: Water content was determined by thermal gravimetric analysis (TGA7, Perkin–Elmer). Infrared spectra were recorded on a Magna 550 Nicolet spectrophotometer, by using KBr pellets. NMR measurements were performed on a Bruker Avance 300 or a Bruker Avance 400 spectrometer, operating at 300 or 400 MHz, respectively, in 5 mm tubes. Chemical shifts were referenced to the usual external TMS standard. Diffusion experiments were recorded at 400 MHz-proton-Larmor frequency at RT in D_2O or in $[D_6]$DMSO. The sequence corresponded to the Bruker pulse program ledpgp2s[40] by using stimulated echo, bipolar gradients, and longitudinal eddy current delay as z filter.

 © 2007 Wiley-VCH Verlag GmbH & Co. KGaA, Weinheim

The four 2-ms gradient pulses had sine bell shapes and amplitudes ranging linearly from 2.5 to 50 G cm^{-1} in 32 steps. The diffusion delay was 100 ms and 16 scans were made. The processing was done by using a line broadening of 5 Hz and the diffusion rates calculated by using the Bruker processing package. The tubes were prepared by dissolving an equimolar mixture of the sample x with the reference sample (r) (approximately 5–10 mg of each compound) in 750 μL of D_2O or DMSO. The auto-diffusion coefficients of each species were measured three times or more to obtain a satisfactory average value for the D_r/D_x ratio. For NMR titrations, tubes with different ratios ligand/molybdenum wheels were obtained by mixing various quantities of solutions of ligand in D_2O with 1 mL of a solution of $K_{2-x}(NMe_4)_x[I_2Mo_{10}O_{10}S_{10}(OH)_{10}(H_2O)_5]$ (corresponding to about 10 mg of this compound) in D_2O. The resulting suspension was stirred and left standing overnight before analysis.

X-ray crystallography: Structures of anionic complexes $[Mo_{12}\text{-TerP}]^{2-}$, $[Mo_{16}(PDA)_2]^{4-}$, and $[Mo_{16}(IsoP)]^{4-}$ were obtained from single crystals of $Cs_2[Mo_{12}TerP]$, $Cs_4[Mo_{16}(PDA)_2]$, and $(NMe_4)_4[Mo_{16}(IsoP)_2]$, respectively. The latter three were air-sensitive and were mounted in capillaries. Dimensions of crystals and cell parameters are given in Table 1. Note that the number of solvates in the structures of these three compounds is higher than that found by TGA and elemental analysis. On exposure to air, the solvate molecules evaporated spontaneously. In the case of $Cs_2[Mo_{12}TerP]$, DMF molecules were progressively replaced by water-in-air. X-ray intensity data were collected at RT on a Bruker Nonius X8-APEX2 CCD area detector diffractometer by using $Mo_{K\alpha}$ radiation ($\lambda =$ 0.71073 Å). Data reduction was accomplished by using the SAINT V7.03 program (APEX2 Version 1.0-8; Bruker AXS, Madison, WI, 2003). The substantial redundancy in data allowed a semi-empirical absorption correction (SADABS V2.10) to be applied on the basis of multiple measurements of equivalent reflections. The structure was solved by direct methods, developed by successive difference Fourier syntheses, and refined by full-matrix least-squares on all F^2 data by using SHELXTL V6.12 (SHELXTL Version 6.12; Bruker AXS, Madison, WI, 2001). Crystallographic data are reported in Table 1, selected bond lengths and angles are given in Tables S1 and S2, respectively, in the Supporting Information. For the three compounds, hydrogen atoms were included in calculated positions and allowed to ride on their parent atoms. CCDC-620095, CCDC-620096, and CCDC-620097 contain the supplementary crystallographic data for this paper. These data can be obtained free of charge from the Cambridge Crystallographic Data Centre via www.ccdc.cam.ac.uk/data_request/cif. Figures 1, 2, and 3 were generated by Diamond Version 3.0c (copyright Crystal Impact GbR).

Syntheses: $K_{2-x}(NMe_4)_x[I_2Mo_{10}O_{10}S_{10}(OH)_{10}(H_2O)_5]\cdot 20H_2O$ $(0 < x < 0.5)$ was prepared as described in literature and characterized by routine methods. Terephtalic acid, isophtalic acid, and phenylenediacetic acid were purchased from Aldrich Chemicals.

$Cs_2[Mo_{12}O_{12}S_{12}(OH)_{12}(C_8H_4O_4)]\cdot 15H_2O\cdot 6DMF$, $Cs_2[Mo_{12}\text{-TerP}]$: To terephtalic acid (100 mg, 0.6 mmol) in suspension in water (10 mL), was added molar KOH (1.2 mL, 1.2 mmol). The resulting colorless solution of terephtalate was then mixed with $K_{2-x}(NMe_4)_x[I_2Mo_{10}O_{10}S_{10}(OH)_{10}(H_2O)_5]\cdot 20H_2O$ (1 g, ca. 0.4 mmol) in water (30 mL). The pH was adjusted to 5 with 1 M potassium hydroxide and the mixture was stirred at 50 °C for 45 min. The solution was cooled down to room temperature, and the yellow precipitate (less than 50 mg) was removed by centrifugation (NMe_4^+ salt of $[Mo_{12}TerP]^{2-}$). A large excess of CsCl was finally added (1 g, 6 mmol) to precipitate $Cs_2[Mo_{12}TerP]\cdot xH_2O$ (870 mg, yield 92 %). ^{1}H NMR ([D$_6$]DMSO): $\delta = 11.43$ (s, 4H), 10.56 (s, 8H), 5.07 ppm (s, 4H); IR (KBr pellet, see Figure S8 in the Supporting Information): $\tilde{\nu} = 1617$(s), 1540(s), 1382(s), 966(s), 530(s) cm^{-1}. This crude product (200 mg) was then dissolved in a DMF/water (20 mL, 1:1) mixture and the resulting solution was allowed to evaporate slowly in air. After few days, single crystals of $Cs_2[Mo_{12}O_{12}S_{12}(OH)_{12}(C_8H_4O_4)]\cdot 2H_2O\cdot 12DMF$ were obtained as air-sensitive yellow needles. After several crystals were removed for X-ray study, the crystals were isolated by filtration, washed with water, and dried in air. ^{1}H NMR ([D$_6$]DMSO): $\delta = 11.44$ (s, 4H), 10.58 (s, 8H), 7.96 (s, DMF), 5.07 ppm (s, 4H); ^{1}H NMR (D_2O): $\delta = 7.81$ (s, DMF), 5.18 (s, aromatic protons of ligand $TerP^{2-}$), 2.90 ppm (s, DMF), 2.74 ppm (s, DMF). From integration, the amount of lattice DMF has been estimated at about 6 DMF molecules per molecular complex $Cs_2[Mo_{12}O_{12}S_{12}(OH)_{12}(C_8H_4O_4)]$. IR (KBr pellet, see Figure S9 in the Supporting Information): $\tilde{\nu} = 1644$(s), 1543(s), 1496 (m, DMF), 1436 (m, DMF), 1378 (s), 1252 (mw, DMF), 1106 (s, DMF), 972 (s), 924 (s), 557 cm^{-1} (s); elemental analysis calcd (%) for $Cs_2[Mo_{12}O_{12}S_{12}(OH)_{12}(C_8H_4O_4)]\cdot 15H_2O\cdot 6DMF$ ($M =$ 3070.9 g mol^{-1}): C 10.17, H 2.89, N 2.73, S 12.53, Mo 37.49; found: C 10.40, H 2.60, N 2.73, S 12.86, Mo 36.94; EDX atomic ratio calcd (found): Mo/S = 1 (1.12); Mo/Cs = 6.00 (6.48); S/Cs = 6 (5.79).

$Rb_4[Mo_{16}O_{16}S_{16}(OH)_{16}(H_2O)_4(C_{10}H_8O_4)_2]\cdot 20H_2O$, $Rb_4[Mo_{16}(PDA)_2]$: To phenylenediacetic acid (H_2PDA) (80 mg, 0.4 mmol) in suspension in water (5 mL), was added molar sodium hydroxide (0.8 mL, 0.8 mmol). The resulting solution was then added to $K_{2-x}(NMe_4)_x[I_2Mo_{10}O_{10}S_{10}(OH)_{10}(H_2O)_5]\cdot 20H_2O$ (1 g, ca. 0.4 mmol) in suspension in water (25 mL). The pH was adjusted to 4.5 with NaOH (1 M) and the mixture was heated at 50 °C for 30 min under stirring. The obtained suspension was centrifuged to remove some yellow precipitate, and RbCl (200 mg, 1.65 mmol) was added to the filtrate. After one day, 420 mg of crystals suitable for X-ray diffraction study were collected by filtration (yield 56 %), were washed with water, and dried in air. ^{1}H NMR (D_2O): $\delta = 5.85$ (d, $J = 8$ Hz, 2H, aromatic protons), 5.69 (d, $J = 8$ Hz, 2H), 1.58 (s, 2H), 0.70 ppm (s, 2H); IR (KBr pellet, see Figure S10 in the Supporting Information): $\tilde{\nu} = 1546$(s), 1425 (m), 1394(s), 947(s), 509 cm^{-1} (s); TGA: Loss of about 24 water molecules between room temperature and 150 °C corresponding to twenty lattice water molecules and four coordinated aquo ligands of the molybdenum ring; elemental analysis calcd (%) for $Rb_4[Mo_{16}O_{16}S_{16}(OH)_{16}(H_2O)_4(C_{10}H_8O_4)_2]\cdot 20H_2O$ ($M =$ 3735 g mol^{-1}): C 6.43, H 1.67, Rb 9.15, S 13.74, Mo 41.10; found: C 6.45, H 2.16, Rb 9.16, S 13.69, Mo 41.10; EDX atomic ratio calcd (found): Mo/S = 1.00 (1.10); Mo/Rb = 4.00 (4.39); S/Rb = 4.00 (3.97).

$Cs_4[Mo_{16}O_{16}S_{16}(OH)_{16}(H_2O)_4(C_{10}H_8O_4)_2]\cdot 18H_2O$, $Cs_4[Mo_{16}(PDA)_2]$: To phenylenediacetic acid (H_2PDA) (48 mg, 0.25 mmol) in suspension in water (20 mL) was added molar sodium hydroxide (0.5 mL, 0.5 mmol). The resulting solution was then added to of $K_{2-x}(NMe_4)_x[I_2Mo_{10}O_{10}S_{10}(OH)_{10}(H_2O)_5]\cdot 20H_2O$ (0.5 g, ca. 0.2 mmol) in suspension in water (25 mL). The pH was adjusted to 4.5 with NaOH (1 M) and the mixture was heated at 50 °C for 15 min under stirring. After cooling, caesium nitrate (100 mg, 0.5 mmol) was added, and the solution was kept in air. After several days, 50 mg of single crystals suitable for X-ray diffraction were obtained (yield around 5 %). ^{1}H NMR (D_2O): $\delta = 5.85$ (d, $J = 8$ Hz, 2H), 5.69 (d, $J = 8$ Hz, 2H), 1.59 (s, 2H), 0.70 ppm (s, 2H); IR (KBr pellet, see Figure S11 in the Supporting Information): $\tilde{\nu} =$ 1543(s), 1424 (m), 1392(s), 946(s), 506 cm^{-1} (s); TGA: Loss of about 22 water molecules between room temperature and 150 °C (18 lattice water molecules and four coordinated water molecules) and eight constitutive water molecules (from the sixteen OH bridging groups) between 150 and 350 °C; elemental analysis calcd (%) for $Cs_4[Mo_{16}O_{16}S_{16}(OH)_{16}(H_2O)_4(C_{10}H_8O_4)_2]\cdot 18H_2O$ ($M = 3888.5$ g mol^{-1}): C 6.18, H 1.97; found: C 6.57, H 1.97; EDX atomic ratio calcd (found): Mo/S = 1.00 (1.06); Mo/Cs = 4.00 (3.99); S/Cs = 4.00 (3.78).

$Li_4[Mo_{16}O_{16}S_{16}(OH)_{16}(H_2O)_4(C_{10}H_8O_4)_2]\cdot xH_2O$, $Li_4[Mo_{16}(PDA)_2]$: The lithium salt was prepared from an aqueous solution of the rubidium salt $Rb_4[Mo_{16}(PDA)_2]$ that had been passed through a cation exchange resin in the Li^+ form (Dowex 50WX2). The resultant solutions were evaporated until dryness and the obtained solid was checked by IR, ^{1}H, and ^{13}C NMR. IR and ^{1}H NMR spectra were identical to those of compounds $Rb_4[Mo_{16}(PDA)_2]$ and $Cs_4[Mo_{16}(PDA)_2]$. ^{13}C NMR (D_2O, see Figure S3 in the Supporting Information): $\delta = 176.3$, 175.4, 132.8, 132.6, 130.0, 129.7, 41.5, and 40.4 ppm.

$Rb_4[Mo_{16}O_{16}S_{16}(OH)_{16}(H_2O)_2(C_8H_4O_4)_2]\cdot 28H_2O$, $Rb_4[Mo_{16}(IsoP)_2]$: To isophtalic acid (H_2IsoP) (60 mg, 0.36 mmol) in suspension in water (5 mL) was added sodium hydroxide (180 μL, 0.72 mmol, 4 M). The resulting solution was added to $K_{2-x}(NMe_4)_x[I_2Mo_{10}O_{10}S_{10}(OH)_{10}(H_2O)_5]\cdot 20H_2O$ (0.5 g, ca. 0.2 mmol) in suspension in water (25 mL). The pH was adjusted to 4.5 with NaOH (1 M) and the mixture was heated at 50 °C for 30 min with stirring. After cooling to room temperature, the resulting turbid solution was clarified through centrifugation, and RbCl (200 mg, 1.65 mmol) was added to the orange clear filtrate. A yellow precipitate appeared and was removed by centrifugation. The solution was

 © 2007 Wiley-VCH Verlag GmbH & Co. KGaA, Weinheim

then allowed to evaporate slowly in air. Five days later, air-sensitive orange prismatic crystals were formed. After washing with water, the crystals were dried in air (240 mg, yield 51%). ^{1}H NMR (D_2O): $\delta = 6.45$ (d, $J = 7$ Hz, 2H), 6.20 (t, $J = 7$ Hz, 1H), 6.14 ppm (s, 1H); IR, (KBr pellet, see Figure S12 in the Supporting Information): $\tilde{\nu} = 1610$(s), 1539(s), 1482 (w), 1444(m), 1386(s), 960(s), 941(s), 525 cm^{-1} (s); TGA: Loss of about 38 water molecules between room temperature and 200°C corresponding to 28 lattice water molecules, two coordinated aquo ligands of the molybdenum ring and eight constitutive water molecules (from the sixteen OH bridging groups); elemental analysis calcd (%) for $Rb_4[Mo_{16}O_{16}S_{16}(OH)_{16}(H_2O)_2(C_8H_4O_4)_2]\cdot 28H_2O$ ($M = 3786.8$ g mol^{-1}): C 5.07, H 2.24, S 13.55, Mo 40.54; found: C 5.45, H 2.03, S 13.47, Mo 39.80; EDX atomic ratio calcd (found): Mo/S = 1.00 (1.10), Mo/Rb = 4.00 (3.88), S/Rb = 4.00 (3.53).

$(NMe_4)_4[Mo_{16}O_{16}S_{16}(OH)_{16}(H_2O)_2(C_8H_4O_4)_2]\cdot 18H_2O$, $(NMe_4)_4[Mo_{16}(IsoP)_2]$: To isophtalic acid ($H_2$IsoP) (83 mg, 0.5 mmol) in suspension in water (30 mL), was added molar potassium hydroxide (1 mL, 1 mmol). The resulting solution was added to $K_{2-x}(NMe_4)_x[I_2Mo_{10}O_{10}S_{10}(OH)_{10}(H_2O)_5]\cdot 20H_2O$ (1 g, ca. 0.4 mmol) in suspension in water (10 mL). The pH was adjusted to 4.8 with molar hydrochloric acid and the mixture was heated at 50°C for 15 min with stirring. After cooling to room temperature, a small amount of NMe_4Cl (20 mg, 0.18 mmol) was then added to the previous orange solution and the mixture was kept in air. After several days, 50 mg of single crystals of compound $(NMe_4)_4[Mo_{16}(IsoP)_2]$ were obtained, characterized by X-ray diffraction, isolated by filtration, washed with water, and dried in air (yield 5%). IR (KBr pellet, see Figure S13in the Supporting Information): $\tilde{\nu} = 1596$(s), 1539(s), 1481 (s), 1443(mw), 1384(s), 967 (s), 937(s), 522 cm^{-1} (s); TGA: Loss of about 18 water molecules between RT and 110°C; elemental analysis calcd (%) for $(NMe_4)_4[Mo_{16}O_{16}S_{16}(OH)_{16}(H_2O)_2(C_8H_4O_4)_2]\cdot 18H_2O$ ($M = 3561.3$ g mol^{-1}): C 10.79, H 3.17, N 1.57; found: C 10.71, H 2.78, N 1.72; EDX atomic ratio calcd (found): Mo/S = 1.00 (1.05). No trace of potassium or other alkaline cation was detected.

$Li_4[Mo_{16}O_{16}S_{16}(OH)_{16}(H_2O)_4(C_8H_4O_4)_2]\cdot x H_2O$, $Li_4[Mo_{16}(IsoP)_2]$: The same procedure as that used for the preparation of $Li_4[Mo_{16}(PDA)_2]$ was used, but starting with $Rb_4[Mo_{16}(IsoP)_2]$. FTIR and ^{1}H NMR spectra were identical to that of compound $Rb_4[Mo_{16}(IsoP)_2]$. ^{13}C NMR (D_2O) (see Figure S6 in the Supporting Information): $\delta = 169.9$, 132.5, 131.1, 129.0, 127.1 ppm.

$K_3[Mo_{12}O_{12}S_{12}(OH)_{12}(C_9H_3O_6)]\cdot 22H_2O$, $K_3[Mo_{12}(Trim)]$: $K_{2-x}(NMe_4)_x[I_2Mo_{10}O_{10}S_{10}(OH)_{10}(H_2O)_5]\cdot 20H_2O$ (1 g, ca. 0.4 mmol) was suspended in water (20 mL). Trimesic acid (H_3Trim, 110 mg, 0.5 mmol) in suspension in water (10 mL) was added and the pH was adjusted to 5.5 with KOH (1 M). The resulting solution was heated at 50°C for 45 min. After cooling, the mixture was centrifuged and KCl (1.5 g) was added to the filtrate. After few days, rectangular orange crystals were obtained, isolated by filtration, washed with water, and dried in air. ^{1}H NMR (D_2O): 5.92 ppm (s); ^{1}H NMR ([D_6]DMSO): $\delta = 10.04$ (s, 12H), 5.93 ppm (s, 3H); IR (KBr pellet, see Figure S14 in the Supporting Information): $\tilde{\nu} = 1610$(s), 1544(s), 1438(s), 1370(s), 974(s), 927(s), 531 cm^{-1} (s); TGA: Loss of about 22 lattice water molecules between RT and 270°C, six constitutive water molecules (from the 12 OH bridging groups) between 270 and 430°C and loss of 8% in weight between 430 and 770°C corresponding to the ligand trimesate; elemental analysis calcd (%) for $K_3[Mo_{12}O_{12}S_{12}(OH)_{12}(Trim)]\cdot 22H_2O$ ($M = 2562.8$ g mol^{-1}): C 4.07, H 2.24, K 4.42, Mo 43.39; found: C 4.38, H 2.06, K 4.38, Mo 42.36; EDX atomic ratio calcd (found): Mo/S = 1.00 (1.03), Mo/K = 4.00 (4.07), S/K = 4.00 (3.94).

[1] N. Mizuno, K. Yamaguchi, K. Kamata, *Coord. Chem. Rev.* **2005**, *249*, 1944–1956.
[2] N. Mizuno, M. Misono, *Chem. Rev.* **1998**, *98*, 199–217.
[3] R. Neumann, A. M. Khenkin, *Chem. Commun.* **2006**, 2529–2538.
[4] V. Nardello, J. M. Aubry, D. E. De Vos, R. Neumann, W. Adam, R. Zhang, J. E. ten Elshof, P. T. Witte, P. L. Alsters, *J. Mo . Cata . A* **2006**, *251*, 185–193.
[5] G. Maayan, R. Popovitz-Biro, R. Neumann, *J. Am. Chem. Soc.* **2006**, *128*, 4968–4969.
[6] J. T. Rhule, C. L. Hill, D. A. Judd, *Chem. Rev.* **1998**, *98*, 327–357.
[7] T. Yamase, *J. Mater. Chem.* **2005**, *15*, 4773–4782.
[8] M. Inoue, K. Segawa, S. Matsunaga, N. Matsumoto, M. Oda, T. Yamase, *J. Inorg. Biochem.* **2005**, *99*, 1023–1031.
[9] P. Mialane, A. Dolbecq, F. Sécheresse, *Chem. Commun.* **2006**, 3477–3485.
[10] J. M. Clemente-Juan, E. Coronado, *Coord. Chem. Rev.* **1999**, *195*, 361–394.
[11] A. Müller, F. Peters, M. T. Pope, D. Gatteschi, *Chem. Rev.* **1998**, *98*, 239–271.
[12] D. E. Katsoulis, *Chem. Rev.* **1998**, *98*, 359–387.
[13] A. Müller, S. Roy, *Coord. Chem. Rev.* **2003**, *245*, 153–166.
[14] F. Hussain, U. Kortz, B. Keita, L. Nadjo, M. T. Pope, *Inorg. Chem.* **2006**, *45*, 761–766.
[15] G. Liu, T. B. Liu, S. S. Mal, U. Kortz, *J. Am. Chem. Soc.* **2006**, *128*, 10103–10110.
[16] L. Lisnard, A. Dolbecq, P. Mialane, J. Marrot, E. Codjovi, F. Sécheresse, *Da ton Trans.* **2005**, 3913–3920.
[17] D. L. Long, L. Cronin, *Chem. Eur. J.* **2006**, *12*, 3699–3706.
[18] E. Cadot, M.-A. Pilette, J. Marrot, F. Sécheresse, *Angew. Chem.* **2003**, *115*, 2223–2226; *Angew. Chem. Int. Ed.* **2003**, *42*, 2173–2176.
[19] E. Cadot and F. Sécheresse, *Chem. Commun.* **2002**, 2189–2197.
[20] F. Sécheresse, A. Dolbecq, P. Mialane, E. Cadot, *C. R. Chim.* **2005**, *8*, 1927–1938.
[21] E. Cadot, M. J. Pouet, C. R. Robert-Labarre, C. du Peloux, J. Marrot, F. Sécheresse, *J. Am. Chem. Soc.* **2004**, *126*, 9127–9134.
[22] E. Cadot, B. Salignac, J. Marrot, F. Sécheresse, *Inorg. Chim. Acta* **2003**, *350*, 414–420.
[23] E. Cadot, B. Salignac, T. Loiseau, A. Dolbecq, F. Sécheresse, *Chem. Eur. J.* **1999**, *5*, 3390–3398.
[24] A. Dolbecq, E. Cadot, F. Sécheresse, *Chem. Commun.* **1998**, 2293–2294.
[25] E. Cadot, J. Marrot, F. Sécheresse, *J. C uster Sci.* **2002**, *13*, 303–312.
[26] A. Dolbecq, C. du Peloux, A. L. Auberty, S. A. Mason, P. Barboux, J. Marrot, E. Cadot, F. Sécheresse, *Chem. Eur. J.* **2002**, *8*, 350–356.
[27] S. Floquet, J. Marrot, E. Cadot, *C. R. Chim.* **2005**, *8*, 1067–1075.
[28] B. Salignac, S. Riedel, A. Dolbecq, F. Sécheresse, E. Cadot, *J. Am. Chem. Soc.* **2000**, *122*, 10381–10389.
[29] A. Dolbecq, E. Cadot, F. Sécheresse, *Comptes Rendus Acad. Sci. Ser. II C* **2000**, *3*, 193–197.
[30] J. H. Enemark, J. J. A. Cooney, *Chem. Rev.* **2004**, *104*, 1175–1200.
[31] K. M. Sung, R. H. Holm, *J. Am. Chem. Soc.* **2001**, *123*, 1931–1943.
[32] J.-F. Lemonnier, S. Floquet, A. Kachmar, M.-M. Rohmer, M. Bénard, J. Marrot, E. Terazzi, C. Piguet, E. Cadot, unpublished results.
[33] E. Martinez-Viviente, P. S. Pregosin, L. Vial, C. Herse, J. Lacour, *Chem. Eur. J.* **2004**, *10*, 2912–2918.
[34] E. Terazzi, S. Torelli, G. Bernadinelli, J. P. Rivera, J.-M. Bénech, C. Bourgogne, B. Donnio, D. Guillon, D. Imbert, J.-C. G. Bünzli, A. Pinto, D. Jeannerat, C. Piguet, *J. Am. Chem. Soc.* **2005**, *127*, 888–903.
[35] M. Greenwald, D. Wessely, I. Golberg, Y. Cohen, *New J. Chem.* **1999**, *23*, 337–344.
[36] I. Fernandez, E. Martinez-Viviente, P. S. Pregosin, *Inorg. Chem.* **2005**, *44*, 5509–5513.
[37] A. R. Waldeck, P. W. Kuchel, A. J. Lennon, B. E. Chapman, *Prog. Nuc . Magn. Reson. Spectrosc.* **1997**, *33*, 39–68.
[38] C. S. Johnson Jr., *Prog. Nuc . Magn. Reson. Spectrosc.* **1999**, *34*, 203–256.
[39] M. Pons, O. Millet, *Prog. Nuc . Magn. Reson. Spectrosc.* **2001**, *37*, 267–324.
[40] D. H. Wu, A. D. Chen, C. S. Johnson Jr., *J. Magn. Reson. Ser. A* **1995**, *115*, 260–264.

Received: September 23, 2006
Published online: February 9, 2007

 © 2007 Wiley-VCH Verlag GmbH & Co. KGaA, Weinheim